Наносистеми, наноматеріали, нанотехнології
Nanosistemi, Nanomateriali, Nanotehnologii
2020, т. 18, № 1, сс. 107–124

PACS numbers: 61.46.-w, 62.23.-c, 81.05.Zx, 81.07.-b, 81.16.-c, 82.33.Pt, 83.60.Pq

Modelling the Mechanism of Mineral-Binders' Hydration Processes in a Macro–Micro–Nanosystem

V. N. Derevianko[1], N. V. Kondratieva[2], H. M. Hryshko[3], and M. A. Sanytsky[4]

[1]*Prydniprovs'ka State Academy of Civil Engineering and Architecture, 24-a, Chernyshevsky Str., UA-49600 Dnipro, Ukraine,*
[2]*Ukrainian State University of Chemistry and Chemical Technology, 8 Gagarin Ave., UA-49005 Dnipro, Ukraine*
[3]*Dnipro State Agrarian–Economic University, 25, Serhii Efremov Str., UA-49600 Dnipro, Ukraine*
[4]*Lviv Polytechnic National University, 6, Karpynskoho Str., UA-79013 Lviv, Ukraine*

Today, the topical issue is the development of a model of mineral binders' hydration processes that would allow taking into account the most initial parameters and characteristics, conditions, and the mechanism of the hydration process. Developing this model requires a large amount of information. Most models only allow for the effect of original components. Besides, with the acquired properties, the optimization process becomes complicated due to the increase in a number of models in connection with the application of optimality criteria for the relative properties. Moreover, due to the fact that there is no specified ratio of components topochemically hydrated in the gypsum system under a solution-based scheme, the hydration process becomes more complicated. Thus, to develop the model, we should justify a large number of assumptions. Besides, selecting the optimality criteria by indirect indicators does not give a clear picture of the intended end use of the model. We should also take into account a scaling level and a relationship between the macro-, micro-, and nanoscales. Modelling of mineral binders' hydration processes is presented in the form of a system that changes over time and undergoes macro- to microscale, micro- to nanoscale, nano- to microscale, and micro- to macroscale stages, using a direct model as an example. The transition from a macrosystem and a microsystem to a nanosystem with the formation of a dispersion medium is presented in the form of a surface consisting of nanoparticles in the multidimensional phase space. The surface is the interface between the structural elements and the dis-

persion medium. The second surface is the interface between the dispersion medium and the hardened structure. At the interface, a partial transition from macro- and microsystems to a nanosystem occurs as well as a topochemical reaction of calcium-sulphate transition from hemihydrate to dihydrate. The most high-strength skeleton frame can be developed by adjusting the values of solid surface and crystallization nuclei, which affect the initial three-dimensional structure and the formation of a durable framework. The internal stresses leading to softening of a structure that has not been yet formed do not arise because the blocks' splicing occurs in a free space. Chemical potential is a unit to measure a change in a characteristic function at constant parameters and mass fractions (concentrations) of all substances except the mass fraction (concentration) of a component, the amount of which varies in the system. If the hydration process is topochemical, structure formation rate will be dependent on particle-size distribution and intraparticle diffusion rate.

Актуальною є розробка моделю процесів гідратації мінеральних зв'язувальних речовин, який враховував би значну кількість первинних параметрів і характеристик, умови та механізм процесу гідратації. Для створення такого моделю потрібна значна кількість інформації. Багато моделів враховують вплив тільки вихідних компонентів. Крім того, процес оптимізації за вхідними параметрами ускладнюється через збільшення кількости моделів у зв'язку з використанням в якості критеріїв оптимальності відносних властивостей. Також у зв'язку з тим, що не встановлено співвідношення компонентів, які гідратують у гіпсовій системі за розчинною та топонімічною схемами, зростає складність моделювання процесу гідратації. Тому для створення моделю необхідно обґрунтувати велику кількість допущень. До того ж вибір за непрямими показниками критеріїв оптимальности не дає чіткости уявлення про кінцеву мету призначення моделю. Також потрібно враховувати рівень масштабування, взаємозв'язок макро-, мікро- та нанорозмірностей компонентів. Моделювання процесів гідратації зв'язувальних речовин представлено у вигляді системи, що змінюється в часі та проходить через стадії за схемою макро–мікро–нано–мікро–макро, на прикладі прямої моделі. Перехід макро–мікро в наносистему з утворенням дисперсного середовища представлено у вигляді поверхні, що складається з наночастинок у багатовимірному фазовому просторі. Поверхня є роздільчою межею структурних елементів і дисперсного середовища. Друга поверхня — роздільча межа дисперсне середовище–затвердла структура. На роздільчій межі відбувається частковий перехід макро- та мікросистеми в наносистему, а також топохемічна реакція переходу напівзневодненого гіпсу в двоводний. Створення каркасу з найбільш високою міцністю можна досягти, реґулюючи величину твердої поверхні та центрів кристалізації, які впливають на первинну просторову структуру. Внутрішні напруження, що призводять до пониження міцности ще неутвореної структури, не виникають внаслідок того, що зрощення блоків відбувається у вільному просторі. Мірою зміни характеристичної функції при постійних параметрах і масах (концентраціях) всіх речовин за винятком маси (концентрації) того компонента, кількість якого змінюється в системі, є хемічний потенціял. У разі, коли процес гідратації йде топохемічно, швидкість формування структури буде залежати від ґранулометричного складу компонентів і швидкости дифузії всередині зерна.

Актуальной является разработка модели процессов гидратации минеральных вяжущих веществ, которая бы учитывала значительное количество первоначальных параметров и характеристик, условия и механизм процесса гидратации. Для создания такой модели необходимо значительное количество информации. Многие модели учитывают влияние только исходных компонентов. Кроме того, процесс оптимизации по входящим параметрам усложняется за счёт увеличения количества моделей в связи с применением в качестве критериев оптимальности относительных свойств. А в связи с тем, что не установлено соотношение компонентов, которые гидратируются в гипсовой системе по растворной и топохимической схемам, возрастает сложность моделирования процесса гидратации. Поэтому для создания модели необходимо обосновать большое количество допущений. К тому же выбор по косвенным показателям критериев оптимальности не даёт чёткости представления конечной цели назначения модели. Также необходимо учитывать уровень масштабирования, взаимосвязь макро-, микро- и наноразмерностей компонентов. Моделирование процессов гидратации вяжущих веществ представлено в виде системы, изменяющейся во времени и проходящей через стадии по схеме макро–микро–нано–микро–макро, на примере прямой модели. Переход макро–микро в наносистему с образованием дисперсной среды представлен в виде поверхности, состоящей из наночастиц в многомерном фазовом пространстве. Поверхность является границей раздела структурных элементов и дисперсной среды. Вторая поверхность — граница раздела дисперсная среда–затвердевшая структура. На границе раздела происходит частичный переход макро- и микросистемы в наносистему, а также топохимическая реакция перехода полуводного гипса в двуводный. Создание каркаса с наиболее высокой прочностью можно достичь, регулируя величину твёрдой поверхности и центров кристаллизации, которые влияют на первоначальную пространственную структуру. Внутренние напряжения, приводящие к разупрочнению ещё несформировавшейся структуры, не возникают вследствие того, что срастание блоков происходит в свободном пространстве. Мерой изменения характеристической функции при постоянных параметрах и массах (концентрациях) всех веществ за исключением массы (концентрации) того компонента, количество которого изменяется в системе, является химический потенциал. В случае, когда процесс гидратации идёт топохимически, скорость формирования структуры будет зависеть от гранулометрического состава компонентов и скорости диффузии внутри зерна.

Key words: hydration, mineral binders, nanosystem, hardened structure, modelling.

Ключові слова: гідратація, мінеральні в'яжучі речовини, наносистема, затвердла структура, моделювання.

Ключевые слова: гидратация, минеральные вяжущие вещества, наносистема, затвердевшая структура, моделирование.

(Received 17 October, 2019)

1. PROBLEM STATEMENT

Currently, levels of development of mineral binders-based construction materials engineering and production technologies (solutions, concretes, *etc.*) pose a challenge of creating models that would allow for the maximum number of initial parameters and properties of components as well as the mechanism and conditions of hydration processes. The research technology (sequence of operations, transition to the nanolevel) mainly consists of two stages: modification of binders during manufacturing and hydration processes (Fig. 1).

In the first variant, in the 'binder–hydration process–hardened system' research scheme, the hydration process in most existing models is described in terms of the 'black box' principle [1]. The disadvantage is that a significant amount of information is required when somewhat setting the hydration process conditions, which is actually impossible to achieve. Moreover, 'composition–property' systems take into account only the impact of initial components; and therefore, the model is not universal. Besides, relative properties (physical, chemical, and mechanical) are used as optimal criteria that increases the number of models and complicates the optimization process for all input parameters. Information about the object using the black box method does not make it impossible to obtain information about internal processes.

$$Y = f\left(x_1, x_2 \ldots x_n\right), \tag{1}$$

where x_1, ..., x_n are impact factors (properties of binder); Y is an output factor (optimization factor).

The same pattern is used in estimating the impact of hydration process conditions. Simplified mathematical model:

$$Y = f\left(z_1, z_2 \ldots z_n\right), \tag{2}$$

where z_1, ..., z_n are impact factors (hydration process conditions); Y is an output factor (optimization factor).

The complexity of the model development is also because the theoretical mechanism of hydration of mineral binders has not been clearly identified. For example, hydration of gypsum systems still has various interpretations. Nevertheless, the most challenging issue is that the ratio of components hydrated under the solution scheme to those hydrated topo-

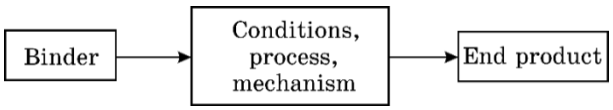

Fig. 1. Process flow diagram of the research.

chemically is not determined. It can also be possible that this ratio varies depending on hydration conditions and properties of hydrating components.

According to the solution scheme, the amount of water should be four times greater than the amount of binder (solubilities of dihydrate and hemihydrate are 2.05 and 8.5, respectively), which is completely not true to the fact [3]. In addition, changing concentrations of the solution and the reversibility of reactions results in additional questions in respect of this scheme.

When considering the process hydration scheme, we can also see a lack of theoretical justification for the process. Since direct attachment of water in inside a particle is caused by diffusion and change in the size of the crystalline lattice.

The process thermodynamics can be presented only in general, *i.e.*, using the total amount of heat released during the hydration of binders' components. The process complexity increases manyfold.

When considering modelling of hydration process, it should be emphasized that when creating a model, you need to justify a large number of assumptions.

The third one is that selecting optimality criteria is performed by indirect indicators: strength, chemical proof, density, *etc.*, which does not give a clear picture of the model's end use. Thus, there should be a particular model for each case. We should also take account of a scaling level and a relationship between macro-, micro-, and nanoscales of components [4].

A reverse model where a structure with optimizing properties is used as an input factor is a more attractive one. In this case, hydration processes and components are the target values, *i.e.*, the nanotechnology approach is used.

In this paper, the authors propose to consider the hydration process as a system whose state changes over time passing macro–micro–nanostages.

Thus, in solving the problems on increasing physical and mechanical properties in modelling, the main challenge is the creation of a universal model of mechanisms of hydration processes of mineral binders to determine the initial components and conditions of interaction thereof. The aim of this article is a modelling of hydration processes of mineral binders in the form of a system that changes over time and undergoes the macro–micro–nano–micro–macro scheme using a direct model as an example.

2. RESULTS AND DISCUSSION

Among gypsum binders, calcium sulphate hemihydrate of the α and β modifications and natural or manufactured anhydrite ($CaSO_4$) with

various impurities are most widely used in construction. Either technical water or natural one containing various salts is used as a grouting fluid. The components are characterized by the structure, density, presence of impurities, and granulometric composition thereof.

It should be noted that the transition of calcium sulphate dihydrate to hemihydrate and anhydrite II occurs at a heat consumption rate as follows [4]:

$$CSH_2 \rightarrow \alpha\text{-}CS\frac{1}{2}H_2 \text{ — } 17.2 \text{ kJ/mole (l) or } 83.7 \text{ kJ/mole (steam);}$$

$$CSH_2 \rightarrow \beta\text{-}CS\frac{1}{2}H_2 \text{ — } 19.4 \text{ kJ/mole (l) or } 85.47 \text{ kJ/mole (steam);}$$

$$CSH_2 \rightarrow \text{CS-anhydrite II — } 16.9 \text{ kJ/mole (l) or } 105 \text{ kJ/mole (steam).}$$

Hemihydrate ($CaSO_4 \cdot 0.5H_2O$) (bassanite) crystallizes in the monoclinic system, and the crystal lattice consists of chains of Ca^{2+} ions and SO_4^{-2} groups located parallel to the C axis forming spatial channels with hydration water therein. Interatomic distances in a hemihydrate are approximately 0.306–0.375 nm, and 0.244 nm in a dihydrate. True density of calcium sulphate hemihydrate is 2.72 g/cm^3 and 2.72 g/cm^3 when transitioning to dihydrate [7].

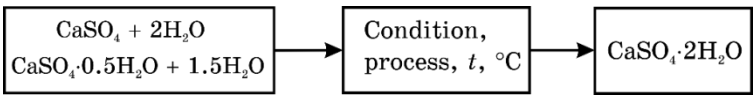

Fig. 2. Overall structure of modelling of hydration process conditions.

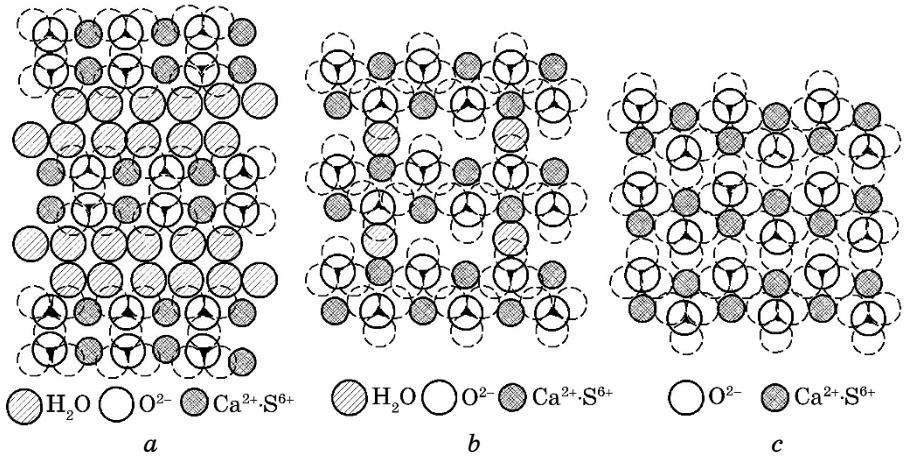

Fig. 3. Structure packing: (*a*) $CaSO_4 \cdot 2H_2O$; (*b*) $CaSO_4 \cdot 0{,}5H_2O$; (*c*) $CaSO_4$ [6].

Crystals in α-hemihydrate are prismatic and well-shaped, while β-hemihydrate has a fibrous and cryptocrystalline structure. Specific surface area of β-$CaSO_4 \cdot 0.5H_2O$ is 2.0 to 2.5 times greater than that of the surface of α-$CaSO_4 \cdot 0.5H_2O$ due to water dispersing and vapour formation between fibres during heat treatment. Anhydrite II has a crystal lattice characterized by the presence of Ca^{2+} chains and SO_4^{-2} groups located parallel to the axis [8].

Modelling of hydration processes is mainly performed using two methods. The first method is used to estimate the effect of the initial components on the properties of the end product (Fig. 1).

In the second method, the first step is developing a model of impact of hydration process conditions and components on the structure of artificial stone and, accordingly, the properties of the hardened system (Fig. 2) is immediately developed.

Physical models can be presented using the following scheme (by Mchedlov-Petrosyan) (Fig. 3) [9].

The structure of gypsum binders and the elemental dihydrate model are shown in Figs. 4, 5.

The presented physical models give us a general idea of the mechanism of hydration of gypsum binders The scheme for cement binders and composite substances is much more complicated due to the multi-component mineralogical composition as well as the time factor having a strong impact.

An important factor is a change in the solution concentration over

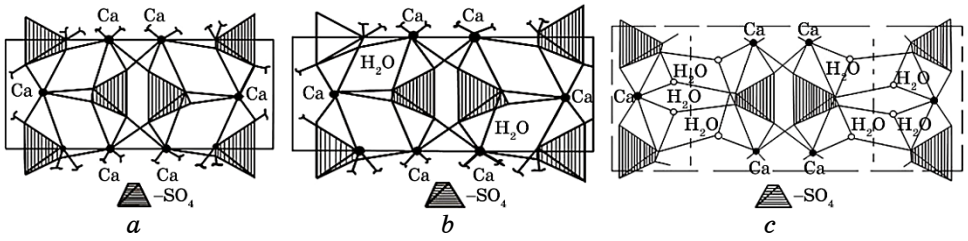

Fig. 4. Structure of gypsum binders: (*a*) $CaSO_4$; (*b*) $CaSO_4 \cdot 0{,}5H_2O$; (*c*) $CaSO_4 \cdot 2H_2O$.

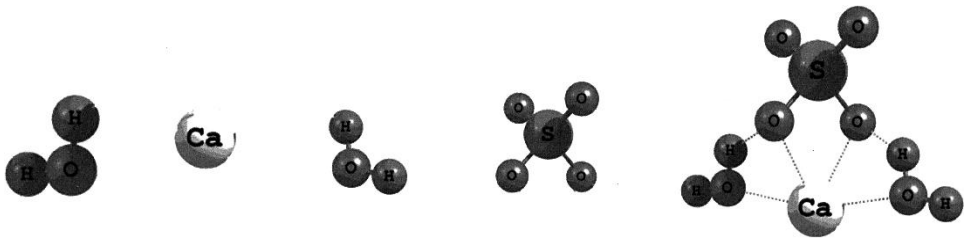

Fig. 5. Elemental calcium sulphate dihydrate model [11].

time and its effect on the hardened structure of binder during hydration. Performed studies of hardening resulting products obtained from calcium sulphate hemihydrate samples unmodified and modified with carbon nanotubes using X'Pert PRO MPD 3040/60 Fa X-ray diffractometer. PANalytical (Freiberg Mountain Academy Technical University, Institute of Ceramics, Glass and Building Materials (IKGB TU Bergakademie Freiberg)) has proven this assumption. The essence of the experiment is to estimate changes in the mineralogical composition in a cyclic mode. Each cycle takes 5 min and 16 sec. The following materials were used as structural models of mineral components for the full-profile quantitative X-ray diffraction analysis: gypsum $CaSO_4 \cdot 2H_2O$ (PDF No. 01-074-1433); bassanite $CaSO_4 \cdot 0.5H_2O$ (PDF No. 01-081-1849); anhydrite $CaSO_4$ (PDF No. 01-086-2270), and carbon C (PDF No. 01-075-2078) [12].

Results of the quantitative X-ray diffraction analysis using the Rietveld method are given in Table.

The x-ray photograph (Fig. 6, Curve *1*) of the gypsum sample at the 1st cycle shows a large amount of both calcium sulphate hemihydrate (24%) and calcium sulphate dihydrate (up to 67%) after 1 hardening cycle. The hydration process is completed at the 18th cycle, *i.e.*, after 95 minutes (Fig. 6, Curve *2*). Main impulses of intensity of the reflected lines of calcium sulphate dihydrate correspond to 6200, 4250, and 3300.

Data from the x-ray photograph of CNT-modified gypsum binder hardening are indicative of the intensification process of the hydration

TABLE. Changes in mineralogical composition, wt.%.

Hardening cycles	$CaSO_4 \cdot 0,5H_2O$	$CaSO_4 \cdot 2H_2O$	$CaSO_4$	Impurities
Mineralogical composition of unmodified calcium sulphate hemihydrate after 1 hardening cycle, Curve *1*, Fig. 6	24	67	4	5
Mineralogical composition of unmodified calcium sulphate hemihydrate after 18 hardening cycles, Curve *2*, Fig. 6	3	88	4	5
Mineralogical composition of modified calcium sulphate hemihydrate after 1 hardening cycle, Curve *1*, Fig. 7	14	77	4	5
Mineralogical composition of modified calcium sulphate hemihydrate after 18 hardening cycles, Curve *2*, Fig. 7	1	93	1	5

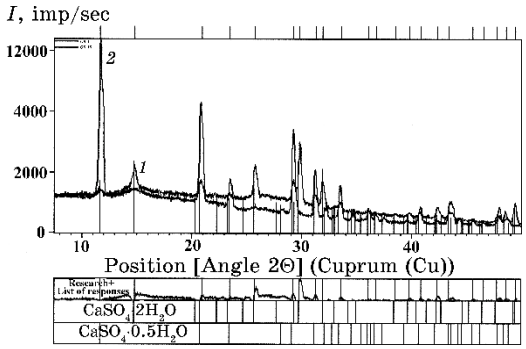

Fig. 6. Rietveld diagram of building gypsum hardening through time G-5: *1*—after the 1st cycle; *2*—after the 18th cycle.

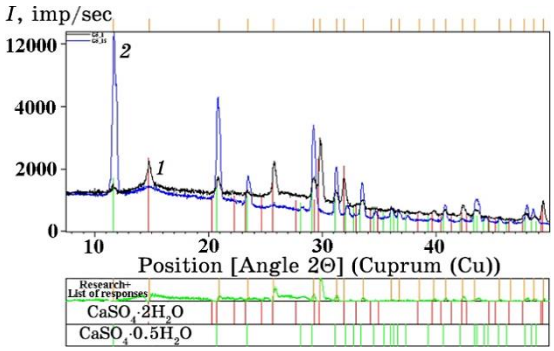

Fig. 7. Rietveld diagram of building gypsum hardening through time G-5: modified with CNTs: *1*—after the 1st cycle; *2*—after the 18th cycle.

processes. The hydration process is also completed at the 18th hardening cycle (upon the expiration of 95 minutes); however, calcium sulphate dihydrate formation rate is considerably higher. The lines of main impulses of calcium sulphate dihydrate correspond to 11300, 9900, 6000 (Fig. 7).

During the hydration of unmodified building gypsum within 18 cycles (95 minutes), the process is running with the formation of $CaSO_4 \cdot 2H_2O$ in the amount of up to 88%. Under the same conditions, the hydration of modified gypsum reaches 93%, and the amount of unreacted $CaSO_4$ even slightly drops (Table).

The follow-up analysis of x-rays photographs shows that, when adding CNTs, the hydration process is intensified and the transition of calcium sulphate hemihydrate to dihydrate is more complete. One of high-impact factors affecting the mechanism of physical and mechanical interactions in a dispersed medium is surface energy that should be taken into account when creating a model.

We see the process of hydration of mineral binders as a system that changes over time and undergoes macro → micro → nano → micro → → macro stages.

At the macro–micro–nanostage, the structure is partially destroyed to nanoscale elements, since the destruction of main impurities (5 to 15% or more) in the binders does not occur.

At the nanostage, new components are formed in the form of amorphous and crystalline phases, followed by the formation of micro- and macrostructures. This representation is also simplified, since the hydration mechanism does not provide for the processes reversibility and constantly changing concentrations of substances in a solution. All the system transformations come down to obtaining a hardened structure with specific properties. The most robust structure of calcium sulphate dihydrate has the characteristics as follow: ρ_0—1.7 g/cm^3, ρ—2.32 g/cm^3, R_{comp}—20 MPa, hardness—2; (x-ray, DTA) crystalline lattice parameters—monoclinic crystal system, $C2/c$, $a = 5.69$ Å, $b = 15.21$ Å, $c = 6.29$ Å, $b = 113.8°$, $Z = 4$ [14, 15].

Major differences in the structures, which affect the properties of a hardened binder, are the presence of pores and the chaotic arrangement of blocks, the structure of blocks and the strength of boundary layers at the microlevel, and the structure of crystalline lattice at the nanolevel.

After gauging with water, binder forms a disperse system characterized by the distribution of solid particles in liquid. Besides, in this case, it is divided into two parts. One part remains unchanged, and the other part is destroyed turning into a nanosystem with further formation of both micro-, macroelements of the end structure.

The nanosystem state at any time interval is characterized by the distribution of nanoparticles $\varphi(\bar{X}_i, \tau)$ and surrounding medium $\Psi(\bar{\xi}, \tau)$ according to the parameters of particles X_i and medium ξ. Therefore, the model should provide for a relationship between the patterns of the environment properties and the distribution of nanoparticles, *i.e.*, the relationship between functions φ and Ψ over time.

Changing the initial state of the environment depending on the macrostate of the original components and the nanocarrier-to-macrosystem ratio (Fig. 8).

The boundary state of the system after the formation of a solution shows partial dissolution of macroparticles of hemihydrate with further transition to dihydrate.

The state of nanoparticles at any time interval τ is determined by

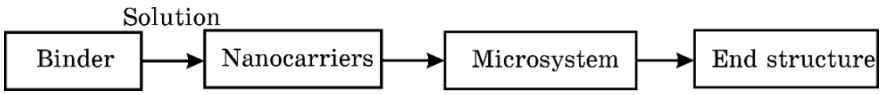

Fig. 8. System state diagram.

mass m, spatial coordinates $\{Y_i\}$, and state parameters for each atom forming a particle, *i.e.*, internal coordinates $\{Z_i\}$. A relationship between the system properties and the external and internal parameters can be expressed as the ratio as follows [17]:

$$\{X_i\} = \{Y_i\},\ \{Z_i\}. \tag{3}$$

In the macro–micro–nanosystem evolution, each element changes from one state to another.

Due to the large number of nanoparticles, the change can be characterized by the probability of transition, P, from state $\{X_0\}$ to state $\{\bar{X}\}$ within time interval $\Delta\tau$.

$$\int_{X_{i0}}^{x_i} \rho d\bar{x}_s = 1. \tag{4}$$

By integrating with respect to all states X_0, the probability function can be calculated as follows:

$$P = \left(\mathbf{X}_i \xi_i\right). \tag{5}$$

Using a known probability function, we can calculate function G_i that characterizes the rate of evolution of the nanosystem [18].

$$G_i = K_G F_i \left(\mathbf{X}_i \xi_i\right), \tag{6}$$

where K_G is the kinetic coefficient; $F_i\left(\mathbf{X}_i \xi_i\right)$ is the elementary-process driving force that is in charge of changes in both the internal X_i and external parameters ξ; G_i is the system evolution function.

According to the model we propose, the transition of a hydrating system from macro- and microstate to a nanosystem with the formation of a dispersed medium can be represented as a surface that consists of nanoparticles in a multidimensional phase space, where the coordinates of the points are the same as the coordinates of the nanoparticles. The surface is the interface between structural elements to which atoms and molecules are attached and a dispersed medium consisting of particular elements, nano-, micro-, and macroparticles. The interaction driving force is a difference in energies of the medium and a degree of saturation of the solution.

$$\xi = C/C_x = 1; \tag{7}$$

C is the concentration of atoms and ions in the medium; C_x is the solubility.

To that extent,

$$G_i = m_0 \sum n_j (P_j - P_j'), \tag{8}$$

where m_0 is the mass of an atom; n_j is the number of structural elements on the surface; P_j' is the probability of detachment of an atom from structural elements per unit of time; P_i is the transition probability function.

Then the kinetic coefficient is as follows:

$$K_G = \sum m_j (P_{j,0} - P_{j,0}'), \tag{9}$$

where $P_{j,0}$ and $P_{j,0}'$ are attachment and detachment of structural elements according to $= 1$.

Thus, the state of a nanosystem can be calculated by calculating the external and internal components, $\psi(\xi, \tau)$ and $Z_i(m, \bar{\xi}_i)$. $\{Z_i\}$ is the elementary density that can be calculated by solving the Schrödinger equation or by means of the external component $\psi(\xi, \tau)$ using techniques of statistical thermodynamics. Both options have significant complications [17].

A large array of experimental data is analysed within the boundaries of models of dissolution deterioration, movement in space, changes in shape, sorption, electrical, and mechanical polarization. In the development of general and particular models, principles of external and internal size effects are used.

For example, the dependence of energy properties of spherical nanoparticles on the size thereof is expressed as the relationship as follows:

$$E = \alpha r^3 + \beta r^2 + \gamma r, \tag{10}$$

where r is the radius of particles; α, β, γ are the constants; αr^3 is a volumetric energy; βr^2 is a surface energy; γr is a surface tension.

Based on the above discussions (Fig. 8) on the structural model of hydration process, the original components of binder after gauging with water form an integrated 'solid matter–dispersed medium' interface, *i.e.*, the total surface area of a solid phase in a dispersed medium (Fig. 9). At the interface, a partial transition of macro- and microsystems to a nanosystem (dissolution of hemihydrate) occurs, insoluble components wetting and a topochemical reaction of calcium sulphate hemihydrate-to-dihydrate transition. The total mass can be used as one of criteria characterizing this surface.

At the initial time interval, the total surface of the solid components consists of the masses as follows:

$$\sum M_{or.comp} = m_1 + m_4 + m_7 + m_{10} + m_{13} + \ldots, \tag{11}$$

where m_1 is the mass of $CaSO_4 \cdot 0.5H_2O$ mass that moves to dihydrate

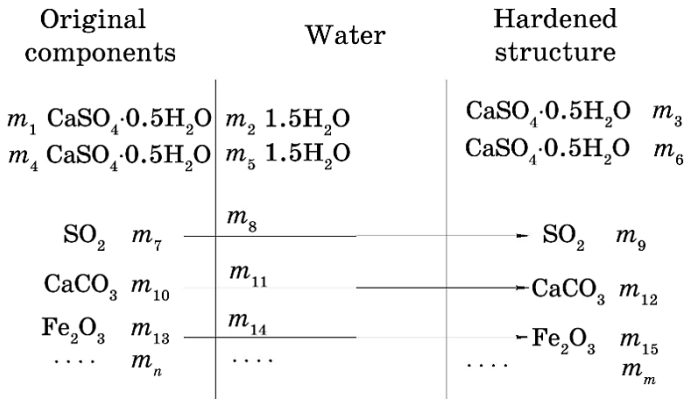

Fig. 9. Hydration process schematic diagram.

under the solution scheme; m_4 is the mass of $CaSO_4 \cdot 0{,}5H_2O$ that topochemically moves to dihydrate; m_7, m_{10}, m_{13}, and m_n are the masses of SO_2, $CaCO_3$, and Fe_2O_3 impurities, *etc.*

The dispersed medium is characterized by changes in concentration of calcium sulphate and insoluble solids. The mass will be as follows:

$$\sum M = (m_1 + m_2) + (m_4 + m_5) + (m_7 + m_8) + (m_{10} + m_{11}) + (m_{13} + m_{14}), \quad (12)$$

where m_2, m_5, m_8, m_{11}, and m_{14} are the masses of water wetting the surface of the binder components.

After reaching the critical concentration, the dispersed medium changes to the end product (in this case, gypsum stone) having the mass as follows:

$$\sum M_{hard.subs} = m_3 + m_6 + m_9 + m_{12} + m_{15}, \quad (13)$$

where m_3, m_6 are the masses of dihydrate; m_9, m_{15} are the masses of impurities; m_{16} is the mass of free moisture.

Changes in the interface of the binder components:

$$\sum S_{sol.comp} = m_1 F_{sp}^1 + m_4 F_{sp}^4 + m_7 F_{sp}^7 + m_{10} F_{sp}^{10} + m_{13} F_{sp}^{13} + \ldots\ldots \quad (14)$$

$$\sum S_{or.comp} = (m_1 F_{sp}^1 + S_b) + (m_4 F_{sp}^4 + S_b) + (m_7 F_{sp}^7 + S_b) + (m_{13} F_{sp}^{13} + S_b) + \\ + \ldots + S_b (m_1 F_{sp}^1 + m_4 F_{sp}^4 + m_7 F_{sp}^7). \quad (15)$$

$$\sum S_{after\ react} = m_3 F_{sp}^3 + m_6 F_{sp}^6 + m_9 F_{sp}^9 + m_{12} F_{sp}^{12} + m_{15} F_{sp}^{15}. \quad (16)$$

The amount of substance on the surface ('solid phase–liquid phase' interface boundary) that reacted topochemically is

$$m_4 F_{sp}^{4\ CaSO_4\cdot 0.5H_2O} + S_b^4 \longrightarrow m_6 F_{sp}^{6\ CaSO_4\cdot 2H_2O} . \quad (17)$$

The surface of binder that reacted under the solution scheme is

$$m_1 F'_{sp} + S'_b \longrightarrow m_3 F_{sp}^{6\ CaSO_4\cdot 2H_2O} . \quad (18)$$

The absence of a time factor and a quantitative ratio of calcium sulphate hemihydrate hydrated under the solution scheme to that hydrated under the topochemical scheme in this model do not allow us to estimate the formation of a gypsum stone structure with certain properties.

As assumed, the initial calcium sulphate hemihydrate hydration reaction occurs on the surface of $CaSO_4\cdot 0.5H_2O + 1.5H_2O \rightarrow CaSO_4\ 2H_2O$ (Fig. 10). Then water at the border with the blocks migrates inwards increasing the internal stress, which leads to the destruction of the blocks.

Presuming that the entire hydration process is topochemical, the subsequent formation of new blocks and a scaffold does not result in the formation of a robust structure. The structure formation rate will depend on the particle size distribution and intraparticle diffusion rate.

To calculate the mass of hydrated substance, we should know the diffusion rate and diffusion depth.

The rate of solubility of calcium sulphate hemihydrate ($CaSO_4\cdot 0.5H_2O$) depends on its properties and adheres to the diffusion rules as follows [21, 22]:

$$dm/d\tau = SD(C_1 - C)/\delta , \quad (19)$$

where $dm/d\tau$ is the amount of substance dissolving per unit of time per unit of volume; D is the diffusion factor; S is the specific surface area of the substance solubility; C_1 is the concentration of the saturated solution; C is the actual concentration; δ is the thickness of the diffusion layer.

A hemihydrate-to-dihydrate transition is determined by the crystallization rate as follows:

$$V = -dC/d\tau = KA\left(C - C_s\right)^2_{\text{solubility}} \quad (20)$$

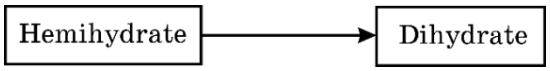

Fig. 10. Hydration process topochemical diagram.

The rate of hydration of mineral binders is determined by the rate of solubility and crystallization.

The sequence of hydration of mineral binders under the solution scheme can be conditionally expressed as follows. At the beginning, the dissolution occurs followed by the formation of a saturated solution, and then, crystallization nuclei and blocks are formed. After that, the blocks fuse together, scaffolds are formed, and finally, voids are filled.

According to suggestions made by A. A. Pashchenko, V. P. Serbin and E. A. Starchevskaya [5], a key factor for strength is a hardening spatial structure that is formed in two stages: the first stage is the formation of a scaffold and the second stage is the scaffold overgrowth or empty space filling.

Thus, we can change the space and the shape and size of crystals by changing the solubility and crystallization conditions.

If the structure of either a hardened binder or materials based thereon is used as an endpoint criterion (output factor), the key parameters should be identified. These parameters can include spatial scaffold, shape of blocks, and crystal morphology.

The key factor for defining these parameters are solutions of a specific concentration, the presence of a solid interface (crystallization nuclei), gauging fluid (water + surfactant), temperature, pressure, and mechanism of transition of calcium sulphate hemihydrate to dihydrate.

According to a number of analyses of structures performed by many researchers, the spatial structure is affected by the initial number of crystallization nuclei and particularly by solid surface area values. These factors have a major impact on the formation of a robust scaffold, because in this case, the intergrowth of blocks occurs in empty space and no additional internal stresses occur. By adjusting both the solid surface value and the number of crystallization nuclei, the highest strength spatial scaffold can be achieved.

The number of crystallization nuclei can be expressed as a solid surface area.

The presence of impurities and particles (F_{hard}) of reacted calcium sulphate hemihydrate increases the solid surface area topochemically and at the same time, macroblocks are formed; in this case, the intergrowth boundaries are characterized by bonds having interaction energy less than 10 kcal/mol, and thus, F_{hard} should be reduced by this value due to the formation of blocks with weak bonds and stresses that are likely to occur.

The sequence of changes in the concentration of the solution, $C_1 < 8.1$, $C_2 = 8.1$, $C_3 < 8.1$, determines the interaction driving force changing from 0 to 1. The maximum concentration of C_2 of 8.1 g/l contributes to the formation of crystallization nuclei, growth and formation of blocks, and voids filling.

The concentration of a solution is a variable increasing from 0 at the beginning of the process to 8.1 g/l within τ_1, then a steady-state concentration stage takes placed followed by the third stage where the concentration is < 8.1 g/l. At this stage, a portion of hemihydrate and water remains unreacted. Studies on determining the presence of calcium sulphate hemihydrate are indicative of this.

Further hydration process is likely to be topochemical.

An increase in the L/S ratio affects the time required to change concentrations C_1 and C_2. Accordingly, the amount of dihydrate obtained under the solution mechanism increases; however, at the same time, the time to reach concentration C_3 increases. This results in the formation of calcium sulphate dihydrate under the topochemical mechanism, yet in the hardened system, which leads to the occurrence of internal stresses reducing the resulting strength.

When C_2 = const, the formation and intergrowth of blocks take place and voids are filled. The ratio of half-periods allows for obtaining crystals of certain morphology and sizes of blocks, and specific voids filling.

It can be assumed that final setting time corresponds to the time of certain formation of a spatial scaffold.

Summarizing this analysis, we would like to combine all the three states as follows: 'components–solution–system hardening'. According to the conventional scheme, the hardened system is considered as a system with certain characteristics: strength, density, porosity, *etc.* According to our model, the hardened system should have a certain structure with specific properties. Characteristics in terms of solution: solid surface, concentration, hydration mechanism, gauging fluid.

A relationship between portions of gauging fluid to the components thereof can be mathematically expressed as follows:

$$Y = f_{h.syst}[\psi_{sol}(Q_{(init)})]; \tag{21}$$

Y is a structure with certain properties; $f_{h.syst}$ is the hardened system function; ψ_{sol} is the solution function; Q is the original components function.

Therefore, changing the intergrowth conditions by adding various additives to a hardening system can affect the shape, size, and number of crystals and, consequently, the formation of a spatial structure to obtain a product with specific properties.

CONCLUSIONS

According to the proposed model, the transition of the macro- and microsystems to a nanosystem with the formation of a dispersed medium can be represented as a surface that consists of nanoparticles in a mul-

tidimensional phase space, where the coordinates of the points are the same as the coordinates of the nanoparticles. The surface is the interface between structural elements to which atoms and molecules are attached and a dispersed medium consisting of particular elements, nano-, micro-, and macroparticles. The interaction driving force is a difference in energies of the medium and a degree of saturation of the solution.

If the entire hydration process is topochemical, the subsequent formation of new blocks and a scaffold does not result in the formation of a robust structure. The structure formation rate will depend on the particle size distribution and intraparticle diffusion rate.

According to the analysis of structures, the robust spatial structure that leads to the formation of a robust scaffold is affected by solid surface area values and the initial number of crystallization nuclei. Because the blocks intergrowth occurs in empty space, no additional internal stresses take place that would result in the softening of a structure that has not yet been formed. By adjusting both the solid surface value and the number of crystallization nuclei, the highest strength spatial scaffold can be achieved.

REFERENCES

1. V. A. Voznesenskyi and T. V. Liashchenko, *ES-modeli v Komp'yuternom Stroitel'nom Materialovedenii* [ES models in Computational Materials Science in Construction] (Odessa: Astroprint: 2006) (in Russian).
2. A. Ye. Kononiuk, *Obobshchyonnaya Teorija Modelirovaniya. Nachala. Kn.1. Ch.1* [Generalized Modelling Theory. Principles. B.1. Pt.1.] (Kyiv: Osvita Ukraiyiny: 2012) (in Russian).
3. P. V. Kryvenko, K. K. Pushkaryova, V. B. Baranovskyy, M. O. Kochevykh, Ye. G. Khasan, B. Ya. Konstantynivskyy, and V. O. Raksha, *Budivel'ne Materialoznavstvo: Pidruchnik* [Materials Science in Construction: Textbook] (Ed. P. V. Krivenko) (Kyiv: Lira-K: 2015) (in Ukrainian).
4. A. Yu. Zakgeim, *Obshchaya Khimicheskaya Tekhnologiya: Vvedenie v Modelirovanie Khimiko-Tekhnologicheskikh Protsessov: Uchebnoye Posobie* [General Chemical Technology: Introduction to Chemical Process Modeling: Textbook] (Moscow: Logos: 2012) (in Russian).
5. A. A. Pashchenko, V. P. Serbin, and Ye. A. Starchevskaya, *Vyazhushchie Materialy* [Binding Materials] (Kiev: Vysshaya Shkola: 1985) (in Russian).
6. K. K. Pushkariova and M. O. Kochevykh, *Materialoznavstvo dlya Arkhitektoriv ta Dizayneriv: Navchal'nyy Posibnyk* [Materials Science for Architects and Designers: Textbook] (Kyiv: Lira-K: 2018) (in Ukrainian).
7. A. V. Volzhenskiy, Yu. S. Burov, and V. S. Kolokolchikov, *Mineral'nyye Vyazhushchie Veshchestva (Tekhnologiya i Svoistva): Uchebnik dlja Studentov Vuzov* [Mineral Binders (Technology and Properties): Textbook for University Students] (Moscow: Stroyizdat: 1979) (in Russian).
8. P. F. Gordashevskiy and F. V. Dolgoryov, *Proizvodstvo Gipsovykh Vyazhushchikh Materialov iz Gipsosoderzhashchikh Otkhodov* [Production of Gypsum

Binding Materials from Gypsum-Containing Wastes] (Moscow: Stroyizdat: 1987) (in Russian).
9. O. P. Mchedlov-Petrosyan and V. I. Babushkin, *Crystallography*, **6**, No. 6: 933 (1961) (in Russian).
10. W. M. M. Heijnen and P. Hartman, *Journal of Crystal Growth*, **108**: 290 (1991).
11. S. Y. Petrunin, L. V. Zakrevska, and V. Ye. Vaganov, *XXII International Science and Technology Conference Proceedings 'Starodubov Readings. Construction, Materials Science, and Engineering' (April 19–21, 2012, Dnipro)*, Iss. 64: p. 74 (in Ukrainian).
12. V. Derevianko, N. Kondratieva, N. Sanitskiy, and H. Hryshko, *Journal of Engineering Science*, **XXV**, No. 3: 74 (2018); doi: 10.5281/zenodo.2557324.
13. V. Derevianko, N. Kondratieva, and H. Hryshko, *French–Ukrainian Journal of Chemistry*, **6**, No. 1: 92 (2018); https://doi.org/10.17721/fujcV6I1P92-100 (in Ukrainian).
14. L. Kondofesky-Mintova and J. Plank, *Superplasticizers and Other Chemical Admixtures in Concrete: Proceedings Tenth International Conference (October 2012, Prague, Czech Republic)*, p. 423.
15. M. A. Sanytsky, H.-B. Fischer, R. A. Soltysik, and S. W. Korolko, *Internationale Baustofftagung 'ibausil', Tagungsband 1* (2003), p. 0211.
16. V. G. Zavodynskyi, *Komp'yuternoye Modelirovanie Nanochastits i Nanosistem: Spetskurs* [Computer Simulation of Nanoparticles and Nanosystems: Special Course] (Moscow: Fizmatlit: 2013), p. 174 (in Russian).
17 V. M. Kaziev, *Vvedenie v Analiz, Sintez i Modelirovanie Sistem: Uchebnoye Posobie* [Introduction to Analysis, Synthesis and Modelling of Systems. Textbook] (Moscow: Binom. Basic Knowledge Laboratory: 2007) (in Russian).
18. Yu. V. Ustinova, S. P. Sivkov, and V. M. Aleksashin, *Bulletin of MSUCE*, No. 7: 130 (2012); https://cyberleninka.ru/article/v/izuchenie-kristallizatsii-dvuvodnogo-gipsa-v-prisutstvii-polimernyh-dobavok-1 (in Russian).
19. V. V. Belov, A. F. Buryanov, G. I. Yakovlev, V. B. Petropavlovskaya, H.-B. Fisher, I. S. Mayeva, and T. B. Novichenkova, *Modifikatsiya Struktury i Svoistv Stroitel'nykh Kompozitov na Osnove Sul'fata Kal'tsiya: Monografiya* [Modification of the Structure and Properties of Calcium Sulphate-Based Building Composites: Monograph] (Moscow: De Nova: 2012) (in Russian).
20. M. A. Sanytskyi and N. V. Kondratieva, *III All-Ukrainian Science and Technology Conference 'Modern Trends in the Development and Production of Silicate Materials' (September 5–8, 2016, Lviv)*, p. 93 (in Ukrainian).
21. A. F. Gordina, Yu. V. Tokarev, G. I. Yakovlev, Ya. Kerene, and E. Spudulis, *Building Materials*, **2**: 34 (2013) (in Russian).
22. *Fizika i Khimiya Poverkhnosti. Kniga I. Fizika Poverhnosti* [Surface Physics and Chemistry. Book I. Surface Physics] (Eds. M. T. Kartel and V. V. Lobanov) (Kyiv: O. O. Chuiko Institute of Surface Chemistry of the N A.S. of Ukraine–Interservis LLC: 2015) (in Ukrainian).
23. A. G. Chumak, V. M. Derevianko, S. Yu. Petrunin, M. Yu. Popov, and V. Ye. Vaganov, *Nanotechnology in Construction: Online Academic Journal*, No. 2: 27 (2013); http://nanobuild.ru/magazine/nb/Nanobuild_2_2013.pdf.
24. V. N. Derevyanko, A. G. Chumak, and V. E. Vaganov, *Stroitel'nye Materialy*, No. 7: 22 (2014); http://rifsm.ru/u/f/sm_07_14_fin.pdf (in Russian).